

Resonant Slepton Production Yields CMS $eejj$ and $e\cancel{p}_{T,jj}$ Excesses

Ben Allanach,¹ Sanjoy Biswas,² Subhadeep Mondal,³ and Manimala Mitra⁴

¹*DAMTP, CMS, Wilberforce Road, University of Cambridge, Cambridge, CB3 0WA, United Kingdom*

²*Dipart. di Fisica, Università di Roma La Sapienza, Piazzale Aldo Moro 2, I-00185 Rome, Italy*

³*Harish-Chandra Research Institute, Chhatnag Road, Jhusi, Allahabad 211019, India*

⁴*Institute for Particle Physics Phenomenology, Department of Physics, Durham University, Durham DH1 3LE, United Kingdom*

Recent CMS searches for di-leptoquark production report local excesses of 2.4σ in a $eejj$ channel and 2.6σ in a $e\cancel{p}_{T,jj}$ channel. Here, we simultaneously explain both excesses with resonant slepton production in \mathcal{R} -parity violating supersymmetry (SUSY). We consider resonant slepton production, which decays to a lepton and a chargino/neutralino, followed by three-body decays of the neutralino/chargino via an \mathcal{R} -parity violating coupling. There are regions of parameter space which are also compatible at the 95% confidence level (CL) with a 2.8σ $eejj$ excess in a recent CMS W_R search, while being compatible with other direct search constraints. Phase-II of the GERDA neutrinoless double beta decay ($0\nu\beta\beta$) experiment will probe a sizeable portion of the good-fit region.

The recent CMS search for di-leptoquark production found, with a certain set of cuts, a 2.4σ local excess in the $eejj$ channel and a 2.6σ local excess in a $e\cancel{p}_{T,jj}$ channel¹ in comparison to Standard Model (SM) expectations. The CMS searches use pp collision data at the Large Hadron Collider (LHC) and a centre of mass energy of 8 TeV and 19.6fb^{-1} of integrated luminosity. Requiring a certain set of cuts (called ‘ $M_{LQ} = 650$ GeV’ cuts), CMS reported 36 events on a background² of 20.5 ± 3.5 in the $eejj$ channel, and 18 events on a background of 7.5 ± 1.6 in the $evjj$ channel [1]. Taken simultaneously and ignoring correlations between the systematics, these excesses amount to a 3.5σ effect. In addition, a W_R search (with different cuts to the di-leptoquark search) reported a 2.8σ excess in the $eejj$ channel at $1.8 \text{ TeV} < M_{eejj} < 2.2 \text{ TeV}$ [2]. These excesses are not significant enough to claim a discovery, or even evidence. They are similar enough to attempt a unified explanation of all three, and a timely explanation before the next LHC run (Run II) in terms of new physics such that further tests can be applied and analysis strategies can be set for Run II.

There have been a few attempts to explain the CMS excesses with different models. Coloron-assisted leptoquarks were proposed in Ref. [3]. The W_R excess was interpreted in GUT models in Refs. [4, 5]. In Ref. [6], pair production of vector-like leptons was proposed via W'/Z' vector bosons. Ref. [7] performed a detailed analysis (including a general flavor structure) of W'/Z' interpretations of the W_R search data. In ref. [8], it was supposed that leptoquarks consistent with the di-leptoquark excess decay into dark matter particles with a significant branching ratio. Ref. [9] explains the di-leptoquark excesses with di-sbottom production, followed by \mathcal{R} -parity

violating (RPV) decay. In a previous letter [10], we proposed that resonant slepton production was responsible for the W_R search excess in RPV supersymmetry. One of us showed that this explanation is also consistent with recent deviations from SM prediction measured by LHCb in $B^+ \rightarrow K^+ ll$ decays [11].

In the present letter, we shall show that RPV resonant slepton production can simultaneously fit the two excesses in the di-leptoquark search while remaining consistent with other direct searches, including the W_R search data. \mathcal{R} -parity is a multiplicative discrete symmetry defined as $\mathcal{R} = (-1)^{3(B-L)+2S}$, where B and L correspond to baryon and lepton number, and S is the spin. In particular, we show that RPV with a non-zero λ'_{111} coupling can fit the CMS excesses [1, 2] via resonant slepton production (with a left-handed slepton mass of around $m_{\tilde{l}} \sim 2$ TeV) in pp collisions. The slepton (either a selectron or an electron sneutrino) then decays, as shown in Fig. 1, either into $eejj$ or $evjj$. For sleptons much

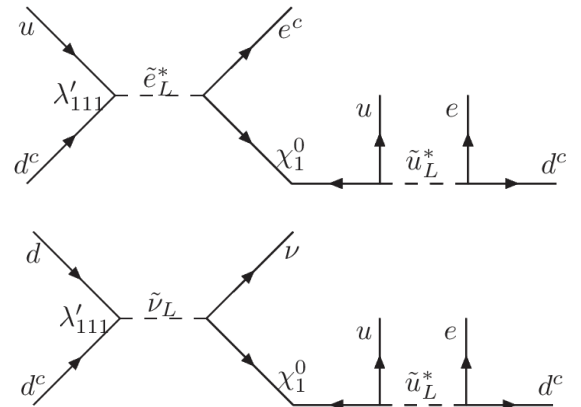


FIG. 1. Feynman diagrams for single slepton production leading to a $eejj(evjj)$ signal at the LHC. Other diagrams, where the χ_1^0 is replaced by χ_1^\pm (among other replacements) also contribute.

¹ CMS refers to this channel as $evjj$, and we shall from here use the same nomenclature.

² We have added systematic and statistical errors in quadrature.

heavier than M_Z , one automatically³ gets cross-sections of the same order of magnitude for the $eejj$ and the $e\nu jj$ channels because their masses are at tree-level related by [12]

$$m_{\tilde{e}_L}^2 = m_{\tilde{\nu}_L}^2 + M_W^2 \cos 2\beta, \quad (1)$$

where $\cos 2\beta < 0$, $\tan \beta$ is the ratio of the two MSSM Higgs doublet vacuum expectation values, and we have neglected small terms proportional to powers of lepton masses. For $m_{\tilde{e}_L}$ around 2 TeV (which we shall be interested in), $m_{\tilde{e}_L} \approx m_{\tilde{\nu}_L}$ is a good approximation. In addition, the parton distribution functions for anti-up quarks u^c and anti-down quarks d^c are similar within the proton, resulting in cross-sections for the two processes shown in Fig. 1 of a similar order of magnitude.

The λ'_{111} term in the RPV superpotential is⁴

$$W_{\mathcal{R}} = \lambda'_{111} L Q d^c. \quad (2)$$

This induces the following Lagrangian terms,

$$\mathcal{L} = \lambda'_{111} \left(-\tilde{e}u d^c - \tilde{u}e d^c + \tilde{d}\nu_e d^c + \tilde{\nu}_e d d^c + \dots \right) \quad (3)$$

The λ'_{111} coupling in Eq. 3 can lead to single slepton production at hadron colliders, as first studied in [18] and subsequently in [19–25]. For an example slepton mass of $m_{\tilde{l}} = 2.1$ TeV and $0.03 < \lambda'_{111} < 0.5$ the production cross-section varies from less than 1 fb to as high as 130 fb [22].

The coupling λ'_{111} responsible for single slepton production in Fig. 1 induces $0\nu\beta\beta$ [13–15], which is not permitted in the SM because of its prediction of lepton number conservation. The present bound on the $0\nu\beta\beta$ half-life of ^{76}Ge is $T_{1/2}^{0\nu} > 2.1 \times 10^{25}$ yrs at 90% CL from GERDA [16], while the 90% CL combined bound on the half-life from previous experiments is $T_{1/2}^{0\nu} > 3.0 \times 10^{25}$ yrs [16]. The future $0\nu\beta\beta$ experiment GERDA Phase-II will be commissioned soon and is expected to improve the half-life sensitivity to $T_{1/2}^{0\nu} \sim 2 \times 10^{26}$ yrs [17]. A positive signal in $0\nu\beta\beta$ experiments is likely to be interpreted in terms of a Majorana nature of the light neutrinos, but instead it could be in part, or dominantly, due to RPV SUSY. There are several contributing diagrams including slepton, neutralino, squark and/or gluino exchange, but for high squark and gluino masses, the dominant one often involves internal sleptons and lightest neutralinos χ_1^0 [10]. As pointed out in Ref. [25], one can then marry resonant slepton search data from the LHC with the predicted $0\nu\beta\beta$ rate in order to provide further tests and interpretations. We shall here neglect contributions

to $0\nu\beta\beta$ coming from neutrino masses, assuming the one due to RPV is dominant.

It is our aim to see if resonant slepton production and decay can fit the CMS di-leptoquark excesses while evading other experimental constraints, and to examine the compatibility with our previous resonant slepton explanation of the W_R excess. Then, we wish to explore the $0\nu\beta\beta$ decay experiments' prospects within any good-fit region. In fact, the strongest indirect bound that is relevant to our analysis is that from $0\nu\beta\beta$. Other indirect bounds on the λ'_{111} coupling can be found in Ref. [26, 27]. For example, the RPV violating contribution to the anomalous magnetic moment of the electron g_e is⁵

$$\delta \frac{g_e - 2}{2} \sim \frac{|\lambda'_{111}|^2 m_e^2}{32\pi^2 \tilde{m}^2}, \quad (4)$$

where \tilde{m} is the size of supersymmetric particle masses appearing in the one-loop diagram. Putting $\lambda'_{111} = 1$ and $\tilde{m} = 1$ TeV, we obtain a contribution of $< 10^{-15}$, far below current bounds: the difference between the experimental value and the Standard Model prediction is [29] $(-1.06 \pm 0.82) \times 10^{-12}$.

We shall follow a bottom-up phenomenological approach. We decouple sparticles which are not relevant for our hypothesised signals. Otherwise, we fix the first generation lightest neutralino mass $M_{\chi_1^0}$ to be 1 TeV (although we have checked that there are only small deviations in our predictions and constraints if we reduce this to 0.8 TeV) the slepton mass varies from 1.8 TeV up to 2.2 TeV and all other sparticles are above the TeV scale. The squark and gluino masses are fixed at 2.5 TeV. We set other RPV couplings to zero, allowing us to focus purely on the effects of λ'_{111} .

We have considered the following representative scenarios:

S1: $M_1 < M_2 = M_1 + 200 < \mu$, i.e., the LSP is mostly bino-like with a small wino-component. In this case the slepton has a substantial branching ratio of decays to the second lightest neutralino or lightest chargino χ_1^\pm .

S2: $M_1 < \mu < M_2$, the LSP is still dominated by the bino-component, with a heavy intermediate higgsino mass and an even heavier wino mass (> 1 TeV). This case increases the branching ratio of slepton decays into the lightest neutralino and a lepton compared to **S1**.

S3: $M_2 \ll M_1 \simeq \mu$, i.e. the LSP is dominantly wino-like. In this case, slepton decay to χ_1^\pm and χ_1^0 with a substantial branching fraction, which then subsequently decay via λ'_{111} . Depending on the nature of the lightest neutralino and the value of the λ'_{111} coupling, the branching

³ Charged slepton production is larger because it couples to u in the proton rather than the d .

⁴ c denotes the charge conjugate.

⁵ In order to obtain this formula, we converted the approximate expression in Ref. [28] for the anomalous magnetic moment of the muon to that of the electron.

σ_{95}/fb	160	75	50	45	36
$m_{\tilde{l}}/\text{TeV}$	1.8	1.9	2.0	2.1	2.2

TABLE I. 95% upper bound on cross-section times branching ratio times acceptance for resonantly produced sleptons decaying to di-jets [30].

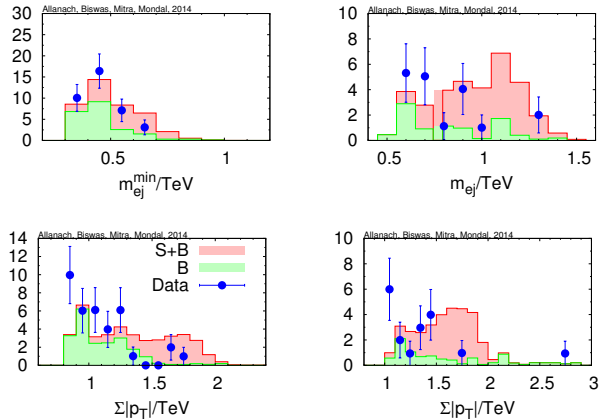


FIG. 2. A comparison of the measured (‘Data’), background (‘B’) and example signal plus background (‘S+B’) distributions for $m_{e_j}^{min}(eejj)$, $m_{e_j}(evjj)$ and the scalar sum of the $p_{T\text{S}}$ of visible objects for (lower left) $eejj$ and (lower right) $evjj$. $m_{e_j}^{min}$ is the invariant mass of the electron-jet pairing combination for which the *difference* between the m_{e_j} for each pair is smallest. The vertical axis measures the number of events falling in a bin after imposing cuts. The signal point corresponds to $\lambda'_{111} = 0.175$, $m_{\tilde{l}} = 2$ TeV and $M_{\chi_1^0} = 0.9$ TeV (S2). Data and SM backgrounds are taken from [1].

ratio changes considerably [23]. At large values of λ'_{111} , the branching ratio of a slepton into two jets becomes larger. Thus, resonant slepton production then becomes constrained by di-jet resonance searches [23]. We take into account the constraint from a CMS di-jet resonance search [30]: the upper limits are displayed in Table I.

We simulate first generation resonant slepton production in pp collisions at a centre of mass energy $\sqrt{s} = 8$ TeV using CalcHEP (v3.4.2) [31], and the subsequent decay, showering and hadronization effects have been performed by PYTHIA (v6.4) [32]. We use SARAH-v4.0.1 [33] and SPheno-v3.2.4 [34] for the model implementation and to compute branching ratios. We approximate the next-to-leading order QCD corrections by multiplying the tree-level production cross section with a K -factor of 1.34 [23]. We use CTEQ6L parton distribution functions [35] with factorization and renormalization scales set at $m_{\tilde{l}}$. To take the detector resolution into account, we also use various resolution functions parameterized as in [36] for the final state objects.

The final states studied in [1], contain either exactly two isolated e s and at least two jets ($eejj$), or one isolated e , at least two jets and missing transverse momentum ($lvjj$). Basic object definitions for the leptons and jets

Channel	Cuts ($M_{LQ} = 650$ GeV)
$eejj$ $evjj$	$S_T > 850$ GeV, $m_{ee} > 155$ GeV, $m_{e_j}^{min} > 360$ GeV, $S_T > 1040$ GeV, $\cancel{E}_T > 145$ GeV, $m_{e_j} > 555$ GeV, $m_T(e\nu) > 270$ GeV
Channel	Cuts ($M_{LQ} = 700$ GeV)
$eejj$ $evjj$	$S_T > 1120$ GeV, $m_{ee} > 160$ GeV, $m_{e_j}^{min} > 390$ GeV, $S_T > 1120$ GeV, $\cancel{E}_T > 155$ GeV, $m_{e_j} > 600$ GeV, $m_T(e\nu) > 280$ GeV
Channel	Cuts
W_R	$m_{ee} > 200$ GeV, $M_{eejj} > 600$ GeV, $2e+ \geq 2j$

TABLE II. Cuts in each channel, from Refs. [1, 2]. $S_T = \sum |p_T|$ is the scalar sum of transverse momenta of all visible objects, m_{ee} is the invariant mass of the lepton pair and $m_{e_j}^{min}$ is the invariant mass of the electron-jet pairing combination for which the *difference* between the m_{e_j} for each pair is smallest. $m_T(e\nu)$ is the electron-neutrino transverse mass, and m_{e_j} is the electron-jet invariant mass where the lepton is paired with the jet that results in the most smallest difference between m_{e_j} and $m_T(e\nu)$.

together with final selection cuts, as outlined in [1], have been imposed as shown in Table II. In their analysis, CMS defined many signal regions, each with its own set of cuts. We pick one of them (designed for 700 GeV dileptoquark sensitivity) which only shows a small excess, to check that our model is not ruled out by it.

We assume a truncated Gaussian for the prior probability density function (PDF) of $\bar{b} \pm \sigma_b$ background events:

$$p(b|\bar{b}, \sigma_b) = \begin{cases} B e^{-(b-\bar{b})^2/(2\sigma_b^2)} & \forall b > 0, \\ 0 & \forall b \leq 0, \end{cases} \quad (5)$$

where B is a normalisation factor that makes the distribution integrate to 1. We marginalise the Poissonian probability of measuring n events over b in order to obtain confidence limits:

$$P(n|n_{exp}, \bar{b}, \sigma_b) = \int_0^\infty db p(b|\bar{b}, \sigma_b) \frac{e^{-n_{exp}} n_{exp}^n}{n!}, \quad (6)$$

where n_{exp} is the number of expected events. The CL of n_{obs} observed events is then $P(n \leq n_{obs})$. Calculated in this way, the $evjj$ excess is a 2.9σ effect, and the $eejj$ excess is a 2.6σ effect, making the two combined 3.9σ . With a two-tailed 95% CL, the number of signal events in the $eejj$ channel is $s_{eejj} \in [19.4, 58.4]$, whereas in the $evjj$ channel it is $s_{evjj} \in [7.8, 34.3]$. For the W_R search, we combine the statistics from the bins $M_{eejj}/\text{TeV} \in [1.6-1.8, 1.8-2.2, 2.2-4]$ (bin $i = 1, 2, 3$, respectively). CMS only observed a large excess in the 1.8-2.2 TeV bin, there was no large excess in the adjacent bins and so these help constrain parameter space. Bin i has a χ^2 statistic $\chi_i^2 = -2 \ln P(n^{(i)}|n_{exp}^{(i)}, \bar{b}^{(i)}, \sigma_b^{(i)})$, where P is obtained from Eq. 6. When considering W_R search constraints, we therefore form a total $\chi^2 = \chi_1^2 + \chi_2^2 + \chi_3^2$. Imposing a 95%CL limit is equivalent to limiting the total $\chi^2 < 3.84$.

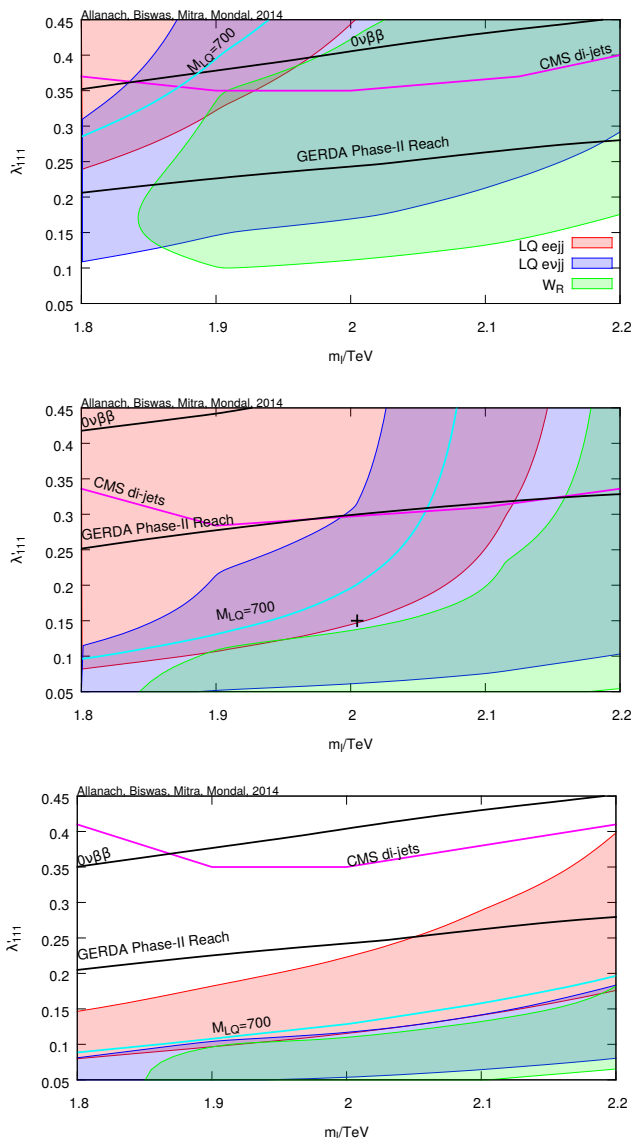


FIG. 3. Constraints in the $m_{\tilde{l}} - \lambda'_{111}$ plane assuming $M_{\chi_1^0} = 0.9$ TeV in scenario (top) **S1**, (middle) **S2** and (bottom) **S3**, where the nuclear matrix elements have been adopted from [24]. The parameter space fitting the $eejj$, $evjj$ di-leptoquark search excesses and the W_R $eejj$ excess to 95%CL is shown in the key. The region above the lines (except for the one labelled ‘GERDA Phase-II Search’ is excluded, labeled near the edge of exclusion: either the 90%CL constraint from current combined neutrinoless double beta decay bounds ($0\nu\beta\beta$) or at the 95%CL exclusion reach from GERDA Phase-II [17] is shown as the region above the solid black line. The cross in the middle panel shows the location of our example point.

We present the predicted event numbers in Table. III and Fig. 2 for an example point in our parameter space and an integrated luminosity of 19.6 fb^{-1} . In Fig. 2, the distributions $m_{e_j}^{min}$, m_{e_j} and the scalar sum of p_T for the visible objects are shown for data [1], background and

Channel	$s + \bar{b}$	$\bar{b} \pm \sigma_b$	Data
$eejj (M_{LQ} = 650 \text{ GeV})$	41.5	20.5 ± 3.3	36
$evjj (M_{LQ} = 650 \text{ GeV})$	33.9	7.5 ± 1.6	18
$eejj (M_{LQ} = 700 \text{ GeV})$	32.7	12.7 ± 2.7	17
$W_R (1.6 < M_{eejj}/\text{TeV} < 1.8)$	12.4	9.6 ± 3.8	10
$W_R (1.8 < M_{eejj}/\text{TeV} < 2.2)$	26.0	4.0 ± 1.0	14
$W_R (M_{eejj}/\text{TeV} > 2.2)$	2.6	2.2 ± 1.8	4

TABLE III. Number of events from signal plus central background $s + \bar{b}$, background b , background uncertainty σ_b and reconstructed data after application of the selection cuts for 19.6 fb^{-1} integrated luminosity and 8 TeV center of mass energy. The signal model is scenario **S2** with $\lambda'_{111} = 0.175$, $m_{\tilde{l}} = 2$ TeV and $M_{\chi_1^0} = 0.9$ TeV. The data and SM backgrounds are taken from Ref. [1] and Ref. [2].

an example signal model point prediction⁶. The figure shows that the distributions are reproduced to a reasonably good level by our model point, although the model point is perhaps slightly broader and of higher energy, compared to the measurements. One must bear in mind though that the statistical power of the kinematical distributions is very limited because of the small statistics.

Fig. 3 shows the $\lambda'_{111} - m_{\tilde{l}_L}$ plane for **S1-S3**. It is evident that the largest values of λ'_{111} that we take are ruled out by the CMS di-jet search [30]. In **S1** and **S2**, there is a small region where all constraints are respected and the three excesses are within their 95%CL constraints. In **S1**, the whole of this region around $\lambda'_{111} = 0.32$ and $m_{\tilde{l}} = 1.88$ TeV can be covered by the GERDA Phase-II [17] $0\nu\beta\beta$ search, whereas in **S2**, it will not cover the overlap region (around $1.9 < m_{\tilde{l}}/\text{TeV} < 2$ and $0.11 < \lambda'_{111} < 0.13$): indeed, much of the parameter space that will be probed by GERDA Phase-II is already disfavored by the CMS di-jets search. The overlap regions we have found in **S1** and **S2** are somewhat marginal, being on the edge of exclusion for all three excess channels. A more thorough search through parameter space (for example considering higher values of $M_{\chi_1^0}$) might make the fit better. There are however large regions where the two di-leptoquark channels both fit data well while respecting other constraints. They are consistent with there being a downward fluctuation in the W_R excess. In **S3**, there is no parameter space where the two di-leptoquark channels give the correct rates, to within a 95% CL. This is because, in **S3**, the chargino has a similar mass to the χ_1^0 and so contributes significantly, producing higher rates for $evjj$ compared to $eejj$. Ideally, one would perform a combined fit between the excesses, taking into account other measurements. However, this

⁶ The kinematic distributions change very little if the slepton mass is varied by 0.1 TeV, whereas the normalisation is sensitive to the overall value of λ'_{111} .

is precluded by the fact that the W_R search and the $eejj$ channels contain common background events, and we do not have access to the correlations between them. For the current paper, we content ourselves with a depiction of where the preferred regions for each measurement lie.

To summarize, the CMS di-leptoquark search excesses are well described by the hypothesis of resonant slepton production. Both the $eejj$ channels and the $evjj$ channel event rates can fit the excess well, and the most important kinematic distributions appear by eye to be reasonable. We have found regions parameter space that are consistent with the 95%CL regions for the di-leptoquark channels and the W_R search.

Acknowledgements: This work has been partially supported by STFC. We thank the Cambridge SUSY working group for stimulating discussions. MM acknowledges partial support of the ITN INVISIBLES (Marie Curie Actions, PITN-GA-2011-289442).

-
- [1] CMS Collaboration, Tech. Rep. CMS-PAS-EXO-12-041, CERN, Geneva, 2014.
- [2] V. Khachatryan *et al.* [CMS Collaboration], arXiv:1407.3683 [hep-ex].
- [3] Y. Bai and J. Berger, arXiv:1407.4466 [hep-ph].
- [4] F. F. Deppisch, T. E. Gonzalo, S. Patra, N. Sahu and U. Sarkar, arXiv:1407.5384 [hep-ph].
- [5] M. Heikinheimo, M. Raidal and C. Spethmann, arXiv:1407.6908 [hep-ph].
- [6] B. A. Dobrescu and A. Martin, arXiv:1408.1082 [hep-ph].
- [7] J. A. Aguilar-Saavedra and F. R. Joaquim, arXiv:1408.2456 [hep-ph].
- [8] F. S. Queiroz, K. Sinha and A. Strumia, arXiv:1409.6301 [hep-ph].
- [9] E. J. Chun, S. Jung, H. M. Lee and S. C. Park, arXiv:1408.4508 [hep-ph].
- [10] B. Allanach, S. Biswas, S. Mondal and M. Mitra, arXiv:1408.5439 [hep-ph].
- [11] S. Biswas, D. Chowdhury, S. Han and S. J. Lee, arXiv:1409.0882 [hep-ph].
- [12] B. C. Allanach, Comput. Phys. Commun. **143**, 305 (2002) [hep-ph/0104145].
- [13] G. Racah, Nuovo Cim. **14**, 322-328 (1937); W. H. Furry, Phys. Rev. **56**, 1184-1193 (1939).
- [14] R. N. Mohapatra, Phys. Rev. **D34**, 3457-3461 (1986); K. S. Babu, R. N. Mohapatra, Phys. Rev. Lett. **75**, 2276-2279 (1995) [hep-ph/9506354].
- [15] M. Hirsch, H. V. Klapdor-Kleingrothaus, S. G. Kovalenko, Phys. Lett. **B352**, 1-7 (1995) [hep-ph/9502315]; M. Hirsch, H. V. Klapdor-Kleingrothaus, S. G. Kovalenko, Phys. Rev. **D53**, 1329-1348 (1996) [hep-ph/9502385]; M. Hirsch, H. V. Klapdor-Kleingrothaus, S. G. Kovalenko, Phys. Rev. **D54**, 4207-4210 (1996) [hep-ph/9603213].
- [16] M. Agostini *et al.* [GERDA Collaboration], Phys. Rev. Lett. **111**, 122503 (2013) [arXiv:1307.4720 [nucl-ex]].
- [17] A. A. Smolnikov [GERDA Collaboration], arXiv:0812.4194 [nucl-ex].
- [18] S. Dimopoulos, R. Esmailzadeh, L. J. Hall and G. D. Starkman, Phys. Rev. D **41**, 2099 (1990).
- [19] J. L. Hewett and T. G. Rizzo, In *Vancouver 1998, High energy physics, vol. 2* 1698-1702 [hep-ph/9809525].
- [20] H. K. Dreiner, P. Richardson and M. H. Seymour, hep-ph/9903419.
- [21] H. K. Dreiner, P. Richardson and M. H. Seymour, hep-ph/0001224.
- [22] H. K. Dreiner, P. Richardson and M. H. Seymour, Phys. Rev. D **63**, 055008 (2001) [hep-ph/0007228].
- [23] H. K. Dreiner and T. Stefaniak, Phys. Rev. D **86**, 055010 (2012) [arXiv:1201.5014 [hep-ph]].
- [24] B. C. Allanach, C. H. Kom and H. Pas, JHEP **0910**, 026 (2009) [arXiv:0903.0347 [hep-ph]].
- [25] B. C. Allanach, C. H. Kom and H. Pas, Phys. Rev. Lett. **103**, 091801 (2009) [arXiv:0902.4697 [hep-ph]].
- [26] R. Barbier, C. Berat, M. Besancon, M. Chemtob, A. Deandrea, E. Dudas, P. Fayet and S. Lavignac *et al.*, Phys. Rept. **420**, 1 (2005) [hep-ph/0406039].
- [27] B. C. Allanach, A. Dedes and H. K. Dreiner, Phys. Rev. D **60**, 075014 (1999) [hep-ph/9906209].
- [28] G. Bhattacharyya, K. B. Chatterjee and S. Nandi, Nucl. Phys. B **831**, 344 (2010) [arXiv:0911.3811 [hep-ph]].
- [29] T. Aoyama, M. Hayakawa, T. Kinoshita and M. Nio, Phys. Rev. Lett. **109**, 111807 (2012) [arXiv:1205.5368 [hep-ph]].
- [30] S. Chatrchyan *et al.* [CMS Collaboration], Phys. Rev. D **87**, no. 11, 114015 (2013) [arXiv:1302.4794 [hep-ex]].
- [31] A. Belyaev, N. D. Christensen and A. Pukhov, Comput. Phys. Commun. **184**, 1729 (2013) [arXiv:1207.6082 [hep-ph]].
- [32] T. Sjostrand, S. Mrenna and P. Z. Skands, JHEP **0605**, 026 (2006) [hep-ph/0603175].
- [33] F. Staub, arXiv:0806.0538 [hep-ph]; Comput. Phys. Commun. **181**, 1077 (2010) [arXiv:0909.2863 [hep-ph]]; Comput. Phys. Commun. **182**, 808 (2011) [arXiv:1002.0840 [hep-ph]].
- [34] W. Porod, Comput. Phys. Commun. **153**, 275 (2003) [hep-ph/0301101]; W. Porod and F. Staub, arXiv:1104.1573 [hep-ph].
- [35] S. Kretzer, H. L. Lai, F. I. Olness and W. K. Tung, Phys. Rev. D **69**, 114005 (2004) [hep-ph/0307022].
- [36] S. Khachatryan *et al.* [CMS Collaboration], JINST **6**, P11002 (2011) [arXiv:1107.4277 [physics.ins-det]]; CMS Collaboration, CMS PAS EGM-10-004; CMS Collaboration, CMS PAS JME-10-014; CMS Collaboration, CMS PAS MUO-10-004.